

Review

Frustrated rare earth magnetism: Spin glasses, spin liquids and spin ices in pyrochlore oxides

John E. Greedan*

*Department of Chemistry and Brockhouse Institute for Materials Research, McMaster University,
ABB 424 and 443, Hamilton, Canada*

Received 30 July 2004; received in revised form 15 December 2004; accepted 15 December 2004
Available online 27 June 2005

Abstract

Rare earth-based materials have played a central role in recent efforts to understand the very unconventional behavior of geometrically frustrated magnetic materials. In particular, rare earth transition metal oxides with the pyrochlore and related structures have been investigated extensively. In the pyrochlore structure both the rare earth and the transition metal sublattices have a topology consisting of corner-sharing tetrahedra and are, thus, geometrically frustrated. Here, we will review progress over the past several years concerning the rare earth titanates, $R_2Ti_2O_7$, which show a remarkable sensitivity to the electronic structure, specifically, the crystal field ground state of the R^{3+} ion. For example, the materials $Gd_2Ti_2O_7$, $Tb_2Ti_2O_7$, $Dy_2Ti_2O_7$ and $Ho_2Ti_2O_7$ exhibit a wide variety of ground states including unconventional long range order (Gd), a spin liquid state (Tb), and spin ice states (Dy, Ho). $Er_2Ti_2O_7$ shows long range order but perhaps by the “order by disorder” mechanism and the $Yb_2Ti_2O_7$ ground state may also be spin liquid like but is presently controversial.

© 2005 Elsevier B.V. All rights reserved.

Contents

1. Introduction	445
2. The pyrochlore structure	445
3. Preliminary comments	446
3.1. The perspective from theory	446
3.2. The experimental situation	446
3.3. $Gd_2Ti_2O_7$ and $Gd_2Sn_2O_7$	447
4. $Tb_2Ti_2O_7$ and $Tb_2Sn_2O_7$	449
5. $Dy_2Ti_2O_7$, $Ho_2Ti_2O_7$, $Ho_2Sn_2O_7$, the spin ices	450
6. $Er_2Ti_2O_7$ and $Er_2Sn_2O_7$	452
7. $Tm_2Ti_2O_7$ and $Tm_2Sn_2O_7$	452
8. $Yb_2Ti_2O_7$ and $Yb_2Sn_2O_7$	452
9. Comment on the stannate series	453
10. Summary and conclusions	454
Acknowledgements	454
References	454

* Tel.: +1 905 525 9140x24725; fax: +1 905 521 2723.
E-mail address: greedan@mcmaster.ca.

1. Introduction

Geometrically frustrated magnetic (GFM) materials have been the focus of intense study over the past several years and a number of reviews exist [1–6]. In addition, three specialist conferences have been held since 2000—Waterloo (Canada) 2000, Santa Fe (2002) and Grenoble (2003). Frustration arises when magnetic sites are subject to competing exchange constraints which cannot be satisfied by simple co-linear orderings. In geometric frustration the competition arises due to the topology of the magnetic sublattice. Frustrated sublattices can be constructed by the condensation of triangles. Indeed, the canonical example is the equilateral triangle with nearest neighbour antiferromagnetic exchange (Fig. 1a), where one-third of the sites are always frustrated, while this fraction is 1/2 for the tetrahedron (four condensed triangles) (Fig. 1b). Triangles and tetrahedra can be condensed by sharing either corners or edges in two or three dimensions and four representative geometrically frustrated lattices are shown in Fig. 2a–d, which include the simple hexagonal net (2D edge-sharing), the Kagome net (2D corner-sharing), the fcc lattice (3D edge-sharing) and the pyrochlore lattice (3D corner-sharing). This list of examples is far from exhaustive. Note that these sublattices are quite familiar ones and it must be stressed that GFM materials occur commonly in nature.

Why are these materials interesting? There are several answers. First, the presence of GF inhibits the formation of long range ordered spin ground states, i.e. the removal of spin entropy, as dictated in principle by the third law of thermodynamics. Secondly, due to the highly local origins of GF, the nominal ground state degeneracy is actually macroscopic, i.e. $\sim N$, where N is the number of magnetic sites and $N \sim 10^{22}$ or so in a real material. While, this degeneracy can be resolved in some cases to give very complex long range order, often, rather exotic short range ordered ground states are found such as spin glasses, spin liquids and spin ices. Finally, it has been realized recently that the issues encountered in the study of GFM materials map closely onto those found in other systems with high levels of degeneracy such as the folding of proteins, for example, or relaxor ferroelectrics.

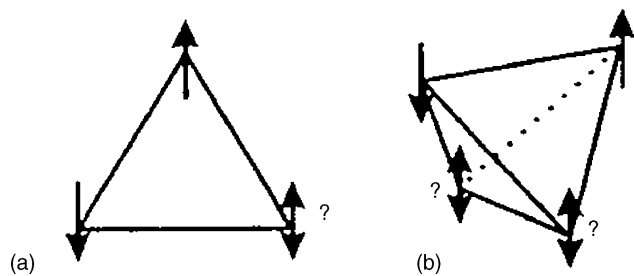


Fig. 1. Geometric frustration as illustrated on a triangular (a) and a tetrahedral (b) plaquette.

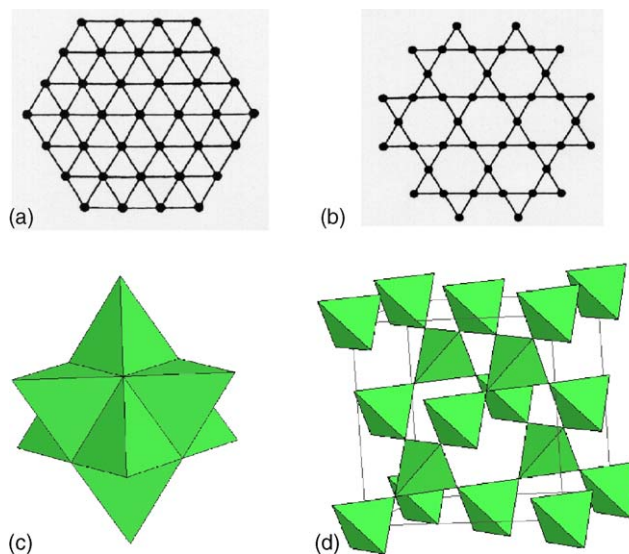


Fig. 2. Geometrically frustrating lattices: (a) edge-sharing triangular; (b) corner-sharing triangular (Kagomé); (c) edge-sharing tetrahedral (face-centered cubic); (d) corner-sharing tetrahedral (pyrochlore).

Central to the study of the GFM phenomenon have been rare earth compounds with the pyrochlore structure. This review will concentrate on the rare earth titanates, $R_2Ti_2O_7$, and to a lesser extent the corresponding stannates, $R_2Sn_2O_7$, where only the rare earth site is magnetic. These materials have been the object of unusually intense study over the past 5 years.

2. The pyrochlore structure

The structure of pyrochlore oxides, $R_2B_2O(1)O(2)_6$, has been described often in the literature [7–9]. The space group is $Fd\bar{3}m$ with R^{3+} in 16d, B^{4+} in 16c, O(1) in 8b and O(2) in 48f. It has become customary to choose the setting with the 16c site at the origin. Both the 16c and 16d sites, separately, form corner-shared tetrahedral, i.e. pyrochlore, sublattices. The smaller B sites are six-fold coordinated by O(2) in a nearly regular octahedral geometry with only a slight trigonal distortion. These octahedra share corners in the manner shown in Fig. 3, resulting in a rather rigid framework of composition B_2O_6 . As a result, the B–O(2)–B angle is in the range of 125° – 135° for most pyrochlore oxides, regardless of the radius of the A-site ion. The A-site, the rare earth site, is coordinated by 6 O(2) and 2 O(1) ions in an unusual geometry. The six O(2) ions form a puckered hexagonal ring, similar to the chair form of cyclohexane, while the two O(1) ions are in linear coordination, i.e. the O(1)–A–O(1) angle is 180° . The orientation of the O(1)–A–O(1) unit is normal to the average plane of the hexagonal ring (see Fig. 4). The A–O(1) bond is unusually short, 2.21 Å in $Gd_2Ti_2O_7$, while the B–O(2) bond is 2.55 Å in the same compound. This imparts a strong axial component to the crystal field at the rare earth site. One final issue, which has become important

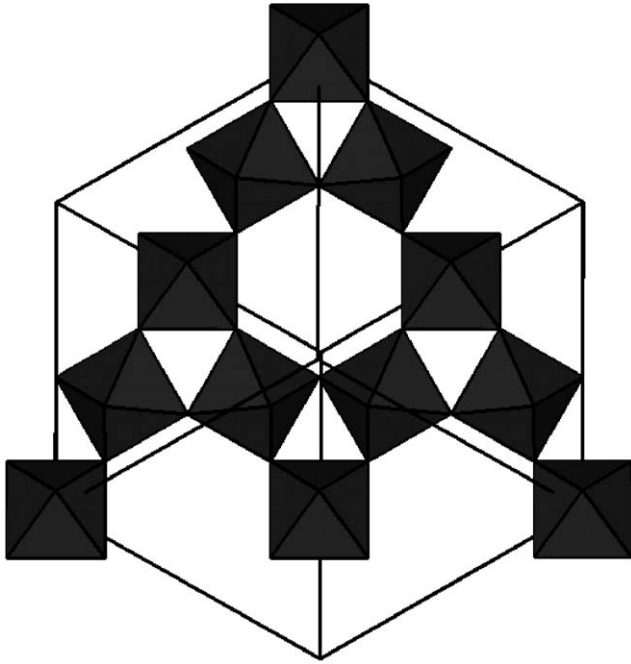


Fig. 3. The network of corner-sharing octahedra of composition BO_3 (B_2O_6) formed in the pyrochlore structure. Note the large hexagonal cavities in which the rare earth ions, R, reside.

recently, is the relationship between the pyrochlore and Kagome lattices. The pyrochlore lattice (16c or 16d sites) can be viewed as a stacking of alternating Kagome and triangular planer sets along $\langle 111 \rangle$ directions in the cubic cells. This is best seen from Fig. 5. Note that the Kagome nets are

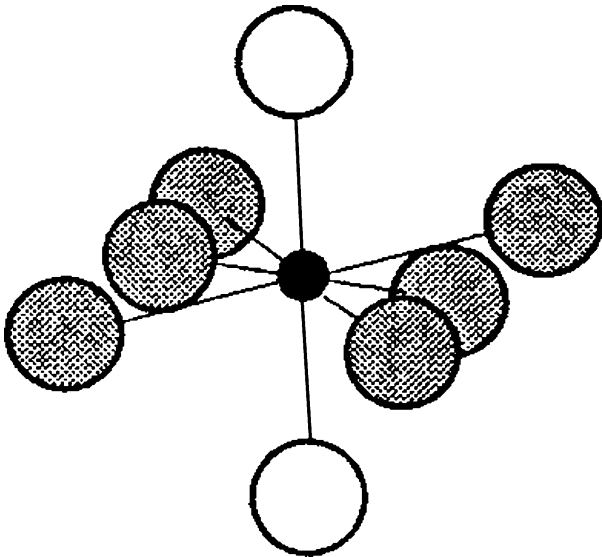


Fig. 4. The local geometry of the rare earth (16d) site in the pyrochlore structure. The O(2) ions (grey spheres) form a puckered six-membered ring about R (small black sphere) with an R–O(2) distance of $\sim 2.5 \text{ \AA}$. The O(1) ions (white spheres) coordinate R in a linear O(1)–R–O(1) unit with a very short R–O(1) distance of $\sim 2.2 \text{ \AA}$.

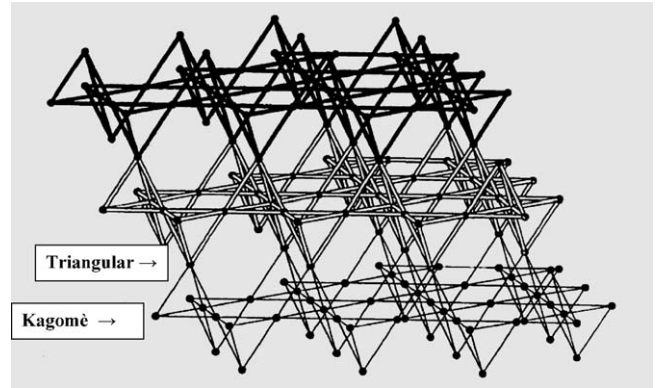


Fig. 5. Stacking of the R-sites (16d) along $\langle 111 \rangle$ directions in the pyrochlore structure showing the Kagome layers alternating with the triangular layers. The nearest neighbor distance within the Kagome sheets is $\sim 3.5 \text{ \AA}$ while the corresponding distance within the triangular sheets is $\sim 7 \text{ \AA}$.

formed from the triangular bases of tetrahedra. Within any Kagome net the apices of the tetrahedra point, alternatingly, up and down, so the layer of sites between two Kagome nets forms an edge-sharing triangular net, also frustrated, but with a site separation twice that within the Kagome nets.

3. Preliminary comments

3.1. The perspective from theory

From both detailed theory and Monte Carlo simulations, it has been shown that for the pyrochlore lattice in the limit of nearest neighbour antiferromagnetic correlations, the system is indeed macroscopically degenerate and no long range spin order is expected for any spin dimensionality at finite temperature [10–12]. Additional perturbations which may include second or higher neighbour exchange, dipole–dipole, applied magnetic fields, thermal or “quantum” fluctuations, disorder, etc. are needed to select a unique ground state. The ordering wave vector of this ground state appears to depend on the details of the perturbation involved. This review will concentrate on the experimental facts, leaving the theoretical situation for others to address.

3.2. The experimental situation

Prior to the late 1990s, few studies existed which addressed the magnetic properties of the titanate pyrochlores. The most extensive were those of Blote and Cashion et al. in which heat capacities and magnetic susceptibilities of several $\text{R}_2\text{Ti}_2\text{O}_7$ phases, among others, were reported [13,14]. These works found evidence for apparent phase transitions near or below 1 K for R = Dy, Ho, Er and Yb, for example. In the following, the current situation for the titanate pyrochlores will be described and comparisons made to the stannates, when possible.

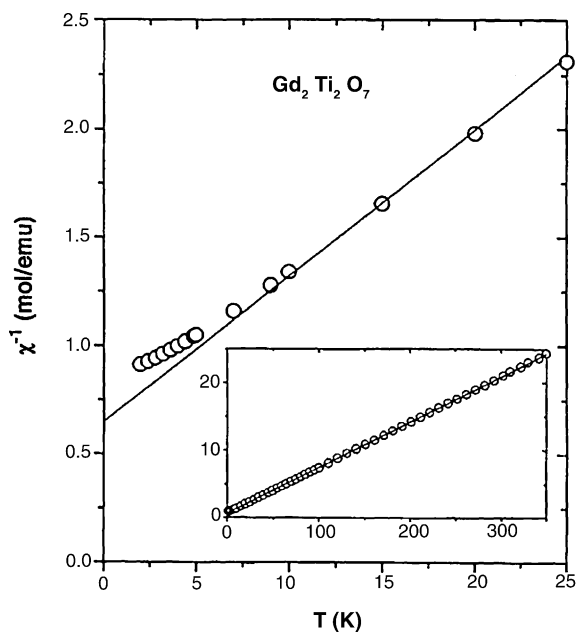


Fig. 6. Susceptibility data for $\text{Gd}_2\text{Ti}_2\text{O}_7$ showing Curie–Weiss behavior to ~ 10 K and no sign of long range order to ~ 1 K [15].

3.3. $\text{Gd}_2\text{Ti}_2\text{O}_7$ and $\text{Gd}_2\text{Sn}_2\text{O}_7$

In principle, Gd^{3+} should represent the simplest case as crystal field and excited multiplet effects are minimized for S-state ions. The bulk susceptibility for $\text{Gd}_2\text{Ti}_2\text{O}_7$ (Fig. 6) follows the Curie–Weiss law to ~ 10 K with $\mu_{\text{eff}} = 7.7 \mu_{\text{B}}$ ($7.94 \mu_{\text{B}}$ for the free ion) and $\theta_{\text{c}} = -9.6$ K [15]. There is no evidence from dc susceptibility of magnetic order down to ~ 1 K. Applying the so-called “frustration index” criterion [3], i.e. $f = |\theta|/T_{\text{c},f}$, one finds $f \sim 10$ which indicates a high level of frustration. Here, T_{c} (T_{f}) is a spin ordering (spin freezing) temperature. θ_{c} sets the energy scale for the magnetic interactions and for non-frustrated systems one expects f to range from 1 to 2 or 3 at the most.

Experiments on a diluted sample $(\text{Y}_{0.98}\text{Gd}_{0.02})_2\text{Ti}_2\text{O}_7$, show that θ_{c} vanishes, essentially [15]. This verifies that any crystal field contribution to θ_{c} can be ignored for this material in accord with expectations.

Nonetheless, it is still necessary to assess the relative contributions of exchange and dipolar interactions to the measured θ_{c} . It is actually a quite complex problem to estimate the dipolar contribution as an infinite lattice sum is involved and the particle shape enters the calculation and a demagnetizing factor must be considered. The best which one can do is to work out upper and lower bounds for the dipolar contribution which is $-2.4 \text{ K} \leq \theta_{\text{c}}^{\text{dip}} \leq 1.2 \text{ K}$ [16]. Thus, the “exchange” component is dominant.

Unequivocal evidence for a phase transition to long range order at 0.97 K is found from specific heat and ac susceptibility data [15]. In fact there are two such transitions in zero applied field, at 0.97 and 0.6 K (Fig. 7, top) [17]. Early reports of a diffuse contribution to the heat capacity appear

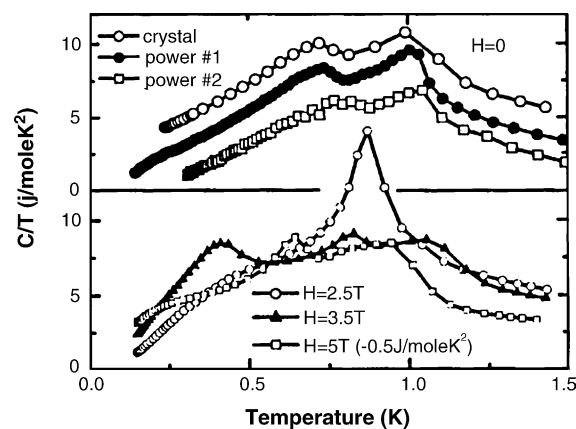


Fig. 7. Presence of two phase transitions in zero applied field at 0.9 and 0.7 K from heat capacity data on $\text{Gd}_2\text{Ti}_2\text{O}_7$ (top). Induction of new transitions in applied fields (bottom) [17].

to have arisen from sample disorder effects [15]. Additional phase transitions are induced in applied fields (Fig. 7, bottom) [17].

The nature of this ordered state, at zero field, has been disclosed using neutron scattering (on $^{160}\text{Gd}_2\text{Ti}_2\text{O}_7$). In the initial study at 50 mK at a spallation source, a $k = (1/2 \ 1/2 \ 1/2)$ structure was found with a most unusual and unexpected spin configuration in which 3/4 of the Gd^{3+} spins are ordered within the Kagome planes, identified earlier in this paper, while 1/4, corresponding to the interplanar sites, remain disordered. This is called a single or 1k structure and is depicted in Fig. 8a [18]. Recent data from a D20 experiment in which a new magnetic reflection, the $(1/2 \ 1/2 \ 1/2)$ reflection, was found have modified this picture [19]. This Bragg peak has finite intensity only if the interplanar sites are also ordered and it appears below 0.7 K, the lower phase transition seen in the specific heat. A detailed analysis of the intensity of this reflection indicates that only partial order ($\sim 27\%$) is present on these sites and a significant diffuse component is seen at $Q = 1.1 \text{ \AA}^{-1}$, indicating that the correlation length of the disordered spins is $\sim 3.5 \text{ \AA}$, the nearest neighbor distance within the Kagomé planes, rather than $\sim 7 \text{ \AA}$, the corresponding distance between the triangular, interplanar sites. The ordered part can be described as 4-k structure depicted in Fig. 8b. Strong diffuse scattering persists above the first T_{c} at 1.4 K, as expected for a magnetically frustrated system and data at higher temperatures would be most welcome. Thus, the origin of the two zero field specific heat anomalies appears to be understood from neutron scattering but the issue of short range magnetic order and its temperature domain await detailed study.

The situation in applied fields is less settled. The normal expectation for materials containing the Gd^{3+} ion is that anisotropy should be unimportant. Nonetheless, recent results from a number of experimental techniques show clearly that this is not the case. For example, the earliest report concerned ESR data on a single crystal which demonstrated

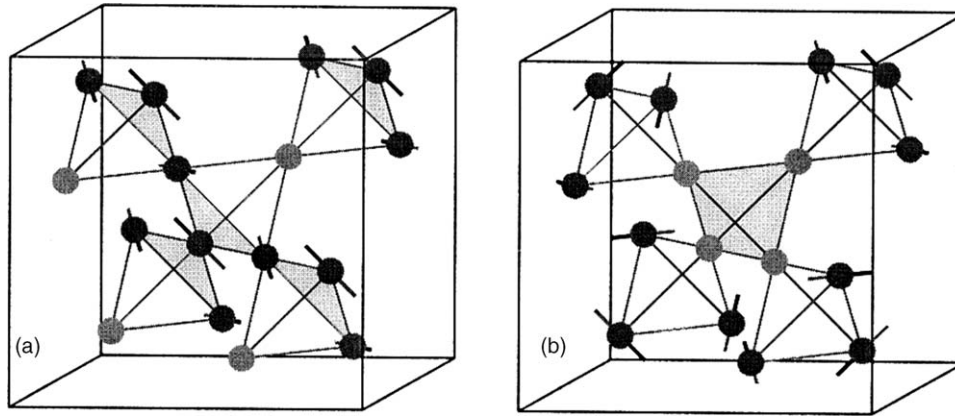


Fig. 8. (a) The 1 k magnetic structure for $\text{Gd}_2\text{Ti}_2\text{O}_7$ which is consistent with the neutron diffraction data above 0.7 K [19]. (b) The 4 k magnetic structure of $\text{Gd}_2\text{Ti}_2\text{O}_7$ consistent with both the Bragg and diffuse neutron diffraction data below 0.7 K [19]. The dark spheres represent Gd ions with a full ($7.0 \mu_B$) ordered moment while the grey spheres carry only a $1.9 \mu_B$ ordered moment.

anisotropy (in the form of two resonance lines) with respect to the $\langle 111 \rangle$ direction at temperatures just below 80 K [20]. This anisotropy becomes very large at 4 K, giving a peak splitting of 4 T, equivalent to ~ 5 K which is of the order of the exchange energy found from the bulk dc susceptibility. This anisotropy was assigned to differences in the exchange interactions effecting the Kagome and interlayer sites. More recently, the H–T phase diagram has been reported for applied fields along three directions, $\langle 111 \rangle$, $\langle 1\bar{1}1 \rangle$ and $\langle 11\bar{1} \rangle$ (Fig. 9) [21]. As well, the authors of [21] performed dc susceptibility measurements on the same single crystals and found essentially no anisotropy, $< 0.2\%$ at any temperature studied. Thus, the origin of the anisotropy seen in the ESR data is still not clear. Anisotropy is also clearly evident in magneto-capacitance experiments [22].

The theoretical situation is also in need of development. No model presently available predicts the phase diagram

of [21], although recent efforts have taken into account dipolar interactions and exchange out to third neighbors [23].

The isostructural stannate, $\text{Gd}_2\text{Sn}_2\text{O}_7$, has received comparatively less attention. The dc susceptibility data indicate $T_c = 1.0$ K and $\theta_c = -9.4$ K, values nearly indistinguishable from the titanate [24]. However, the specific heat shows only a single anomaly at 1.0 K in strong contrast to $\text{Gd}_2\text{Ti}_2\text{O}_7$ [25]. As well, only a single Gd moment is found from ^{155}Gd Mössbauer experiments down to $T < 0.1$ K [25] and μSR indicates a different spin dynamics [26]. All of this suggests a different magnetic structure for the stannate which has yet to be confirmed by neutron scattering. That there should be such distinct differences between two isostructural materials is truly surprising and points up the extreme sensitivity of the ground state to apparently small effects in these highly frustrated materials.

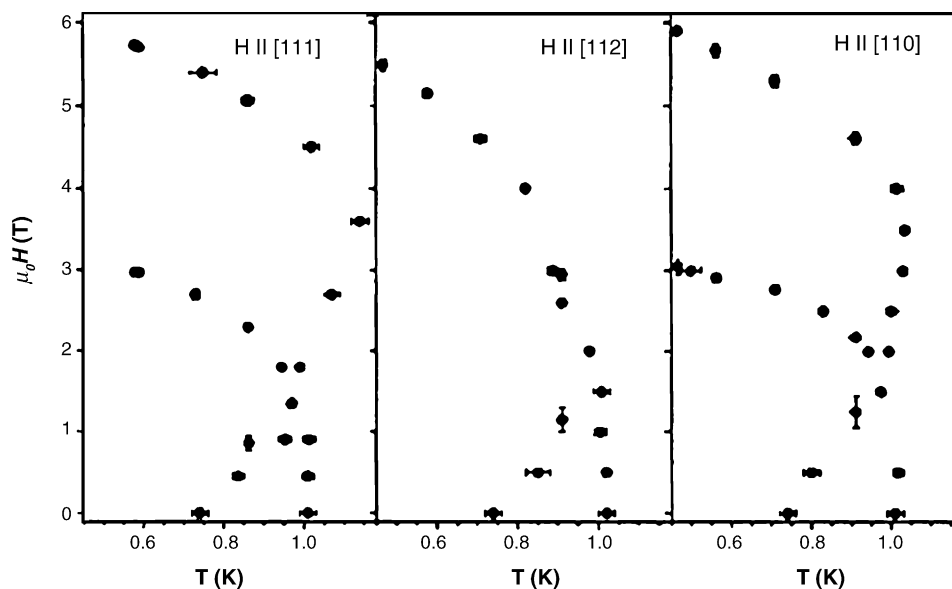


Fig. 9. The H–T phase diagram for a single crystal of $\text{Gd}_2\text{Ti}_2\text{O}_7$ with the field applied parallel to high symmetry directions in the pyrochlore cell [21].

4. $\text{Tb}_2\text{Ti}_2\text{O}_7$ and $\text{Tb}_2\text{Sn}_2\text{O}_7$

Tb^{3+} , $4f^8$, 7F_6 , is an even electron ion and it is difficult to predict, a priori, the single ion properties. For example, a crystal field singlet ground state is not impossible, so a detailed investigation of the single ion properties was carried out using dc susceptibility, specific heat, inelastic neutron scattering and an ab initio calculation of the crystal field at the Tb^{3+} site for $\text{Tb}_2\text{Ti}_2\text{O}_7$ [16,27]. For the pure titanate Curie–Weiss behavior was seen down to about 50 K with a $\mu_{\text{eff}} = 9.6 \mu_{\text{B}}/\text{Tb}^{3+}$ (the free ion value) and $\theta_c = -19$ K. In this case one anticipates that crystal field effects will contribute to θ_c , so a diluted sample, $(\text{Tb}_{0.02}\text{Y}_{0.98})_2\text{Ti}_2\text{O}_7$, was also studied yielding the same $\mu_{\text{eff}}/\text{Tb}^{3+}$ and $\theta_c = -6$ K, which can be taken as the CF contribution, leaving -13 K for the exchange/dipolar part. As the dipolar contribution is at most -2 K, the exchange portion turns out to be nearly the same as that for Gd^{3+} , approximately -10 K. Measurements down to 2 K showed no sign of singlet ground state behavior.

Inelastic neutron scattering data (Fig. 10) indicate the presence of two transitions with weak or no dispersion at 17 and 120 K which can be assigned as crystal field levels. Specific heat results are not inconsistent with this assignment. Various crystal field splitting schemes have been determined from ab initio calculations and from empirical arguments and are in reasonable agreement with the two doublet picture found experimentally as illustrated by the fit to the powder-averaged susceptibility (Fig. 11).

It is important to note that the wavefunctions of both the ground and first excited states are highly Ising-like, being

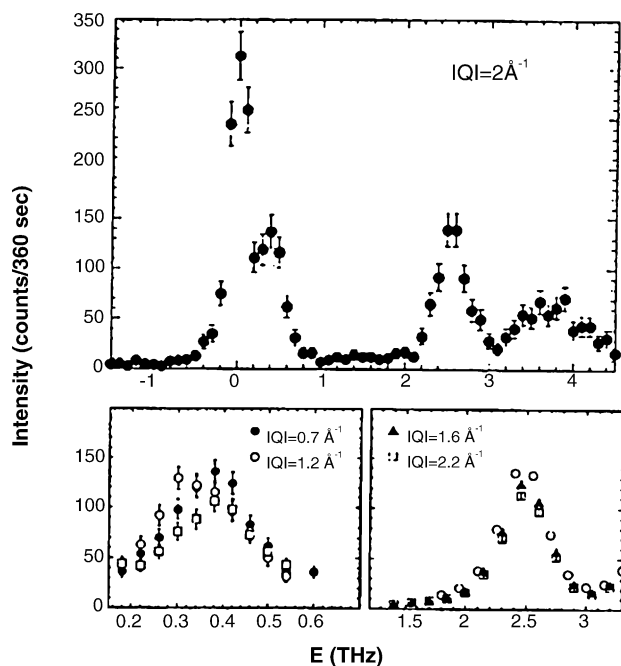


Fig. 10. Inelastic neutron scattering for a powder sample of $\text{Tb}_2\text{Ti}_2\text{O}_7$ showing modes at 0.36 THz (16.8 K), 2.5 THz (120 K) and 3.5 THz (168 K). These are identified as transitions to excited crystal field levels [27,28].

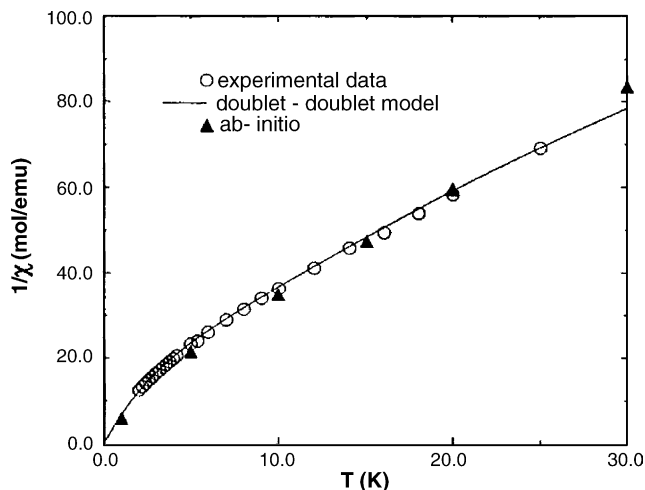


Fig. 11. Fit of the low temperature magnetic susceptibility of $(\text{Y}_{0.98}\text{Tb}_{0.02})_2\text{Ti}_2\text{O}_7$. To a crystal field scheme assuming a doublet structure for both the ground and first excited states derived from ab initio crystal field calculations [16].

comprised of $>90\%$ $M_J = \pm 4$ and $M_J = \pm 5$ for the former and latter, respectively. This is not surprising given the strongly axial nature of the crystal field at the rare earth site in the pyrochlore structure.

While the isostructural gadolinium pyrochlore orders just below 1 K, the initial reports indicated the $\text{Tb}_2\text{Ti}_2\text{O}_7$ does not order in a long range sense down to at least 70 mK. The principal evidence for this was from μSR results which show the persistence of spin dynamics at such a low temperature [27]. This has led to the labeling of this material as either a “cooperative paramagnet” [10] or a spin liquid, the main distinction being that the former term implies classical states while the latter, quantum states. There exists significant evidence, especially from neutron scattering, that strong magnetic correlations exist on a nearest neighbor length scale, $\sim 5 \text{ \AA}$, down to very low temperatures. The earliest studies found an intense diffuse feature centered at $\sim 1.2 \text{ \AA}^{-1}$ and a weaker one near 3.1 \AA^{-1} which persisted, amazingly, up to ~ 100 K [28]. A recent report using the very sensitive neutron spin echo technique, shows the 1.2 \AA^{-1} diffuse peak even at 50 mK [29].

Detection of this effect by NSE also implies that the spins are fluctuating faster than $t \sim 10^{-8}$ s while retaining the short range correlations. The “cooperative paramagnetic” picture is re-enforced by spin dynamics studies of a systematically diluted system, $(\text{Tb}_{1-x}\text{Y}_x)_2\text{Ti}_2\text{O}_7$, where x is varied from 0 to 0.21 (below the percolation limit of 0.39). Both μSR and NSE data show a strong dependence of spin dynamics on x but there is no dramatic change at the percolation concentration, which shows that the interactions are never of infinite range, but involve finite-size clusters [30]. Thus, to date there is no evidence from microscopic probes such as neutron scattering or μSR , for any type of order, either conventional long range order, spin freezing or “spin ice” down to ~ 50 mK at zero magnetic field.

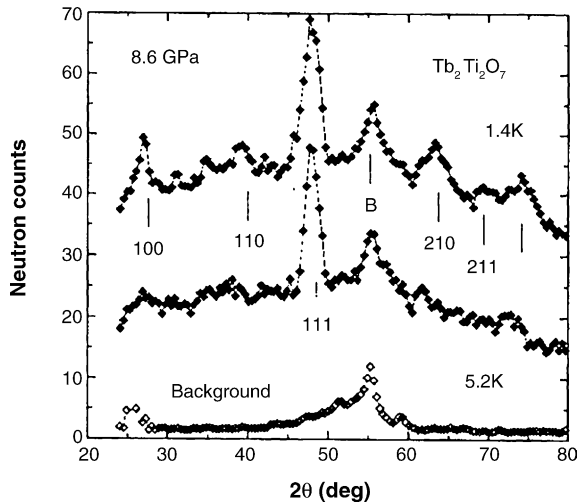


Fig. 12. Pressure-induced, antiferromagnetic long range ordered state at 8.6 GPa and 1.4 K in $\text{Tb}_2\text{Ti}_2\text{O}_7$ [32].

$\text{Tb}_2\text{Ti}_2\text{O}_7$, therefore, appears to be the best realization to date of a spin liquid in three dimensions. Recent theory suggests that the lack of order may be due to the fact that the moment anisotropy in this system is intermediate between an Ising situation and an isotropic one. The fact that the energy scales for the crystal field splittings and the two-ion interactions are comparable may be responsible for the suppression of order [31].

This situation changes under applied pressure or apparently, applied magnetic fields. The situation with pressure is more clearly established and it has been shown that for pressures of 8.6 GPa, a long range ordered, antiferromagnetic state is stabilized with $T_N = 2.1$ K (Fig. 12) [32].

As well, neutron scattering experiments on a single crystal with the applied field along the $\langle 111 \rangle$ direction seem to indicate a strong enhancement of certain Bragg reflections, such as (220) , (224) and (264) , all of which are absent in the zero-field data (Fig. 13) [33]. The magnetic structure has not yet been solved.

Given all of the above evidence for spin liquid behavior, there have been reports which suggest that some form of order does occur. The earliest of these identified a transition at 70 mK below which history dependence was seen in the static susceptibility, not inconsistent with glassy ordering [34]. But the most remarkable report shows very recent data, also on single crystal $\text{Tb}_2\text{Ti}_2\text{O}_7$, including specific heat and ac susceptibility, which seem to suggest magnetic order at temperatures as high as 0.4 K and in zero magnetic field (Fig. 14) [35]. At present, there appears to be no way to reconcile these divergent results.

Typically, $\text{Tb}_2\text{Sn}_2\text{O}_7$ has received scant attention to data, relative to the titanate. The dc susceptibility is similar to the titanate, giving $\theta_c = -12.5$ K. There may be some evidence for ferromagnetic order below 0.87 K but much more work is needed to verify this claim [24].

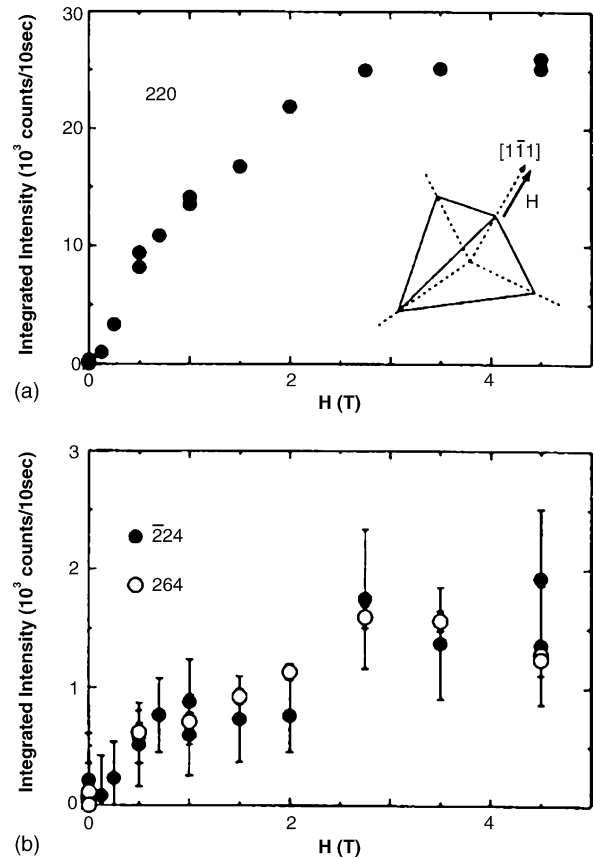


Fig. 13. Magnetic field induced reflections in the neutron elastic scattering for a $\text{Tb}_2\text{Ti}_2\text{O}_7$ single crystal with the field applied parallel to $\langle 111 \rangle$ [33].

5. $\text{Dy}_2\text{Ti}_2\text{O}_7$, $\text{Ho}_2\text{Ti}_2\text{O}_7$, $\text{Ho}_2\text{Sn}_2\text{O}_7$, the spin ices

Dy^{3+} , ${}^6\text{H}_{15/2}$, and Ho^{3+} , ${}^5\text{I}_8$, given such enormous J values, are likely to present complex single ion properties, especially in the strongly axial crystal field at the rare earth site in

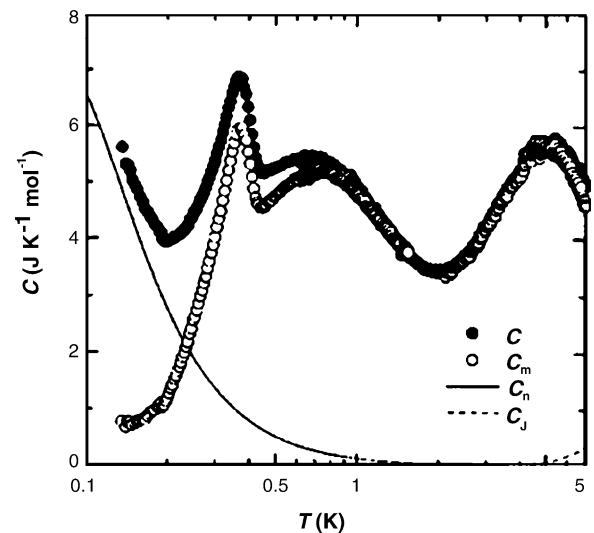


Fig. 14. Apparent specific heat anomalies at zero applied field for $\text{Tb}_2\text{Ti}_2\text{O}_7$ [35].

pyrochlores. The discussion of these materials is best begun with the holmium titanate. The earliest report found a susceptibility maximum near 1 K [14]. Subsequently, a more detailed investigation showed that $\theta_c = 1$ K, much smaller than the values for the gadolinium and terbium titanates which are of order 10 K–20 K and positive, albeit small [36]. It was recognized that the huge Ho^{3+} magnetic moment implied a large demagnetizing field and careful studies correcting for this effect established, eventually, that θ_c was indeed positive, +1.9(1) K. Soon, μSR studies established the absence of long range magnetic order down to 50 mK, again evidence for severe magnetic frustration [37]. Yet, this presents a paradox as the dominant spin–spin coupling is apparently ferromagnetic and it was unclear how a ferromagnet could be subject to geometric frustration. The resolution of this paradox was provided by Harris and Bramwell, in a remarkable insight, by recognizing two facts [38]. Firstly, the crystal field ground state of the Ho^{3+} ion in this material is nearly pure $|J, M_J\rangle = |8, \pm 8\rangle$, i.e. a nearly pure Ising state with quantization axis along (111) . Secondly, with this constraint on the moment directions, the ground state spin structure maps exactly onto the famous problem of the proton configuration in water ice, studied decades ago by Giaque and co-workers [39], Bernal and Fowler [40], and Pauling [41]. This parallel is most easily seen from Fig. 15 which compares the spin configurations within a tetrahedron with spins along the diagonals and the arrangement of protons about an oxygen atom in common water ice in the I_h phase. The four protons about the oxygen atom must form two short (covalent) and two long (hydrogen) bonds while the ferromagnetic spin configuration within the tetrahedron involves two spins pointing out and two spins pointing in. Pauling had shown that the situation for water ice gave rise to a macroscopically degenerate ground state, $\sim(3/2)^{N/2}$, where N is the number of protons in the sample, and an excess or residual entropy, $S \sim (R/2)\ln(3/2)$, found experimentally by Giaque and co-workers [39]. Interestingly, the antiferromagnetic ordering of strongly Ising spins on a tetrahedron is only slightly frustrated as the ground state can be only either all spins out or all spins in.

The first experimental verification of the Harris/Bramwell spin ice conjecture was, interestingly, from specific heat

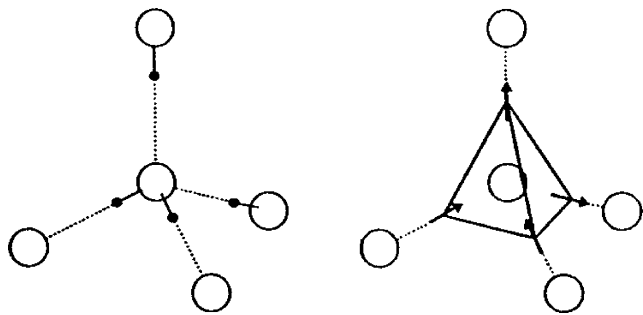


Fig. 15. Analogy between the configuration of ferromagnetic Ising (111) spins within a tetrahedron and the arrangement of protons about oxygen atoms in water ice. The “spin ice” analogy [6].

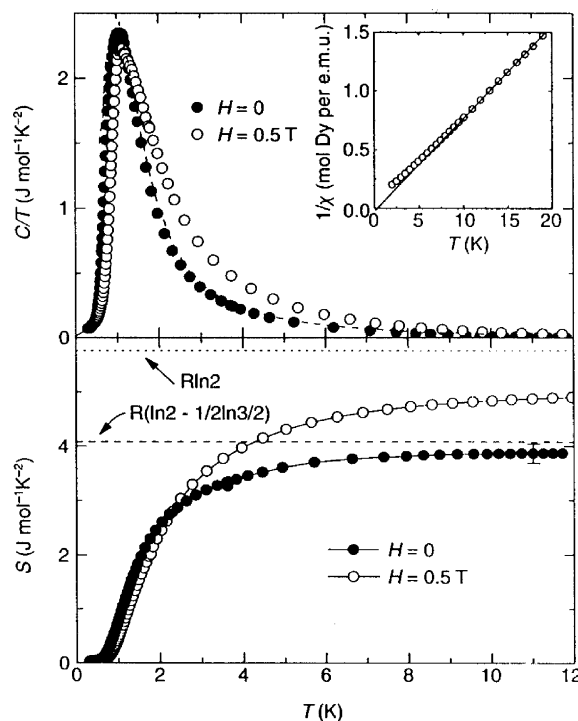


Fig. 16. Specific heat data for $\text{Dy}_2\text{Ti}_2\text{O}_7$ showing the entropy reaching the Pauling spin ice value [42].

studies of $\text{Dy}_2\text{Ti}_2\text{O}_7$ [42]. It had been known for some time that the crystal field ground state for Dy^{3+} in this material was also strongly Ising, especially from magnetization measurements due to Flood [43]. The observed entropy was shown to approach the Pauling value for water ice to within error (Fig. 16). The picture for $\text{Ho}_2\text{Ti}_2\text{O}_7$ was not resolved until a bit later due to the presence in the specific heat of a second, low temperature upturn [44]. Counter to suggestions that this represented spin ordering for holmium titanate, it was shown ultimately to arise from a Schottky anomaly due to the splitting of the nuclear spin levels of ^{165}Ho , as had been shown very early on by Blote for the isostructural $\text{Ho}_2\text{SbGaO}_7$ pyrochlore [13].

One puzzling feature of these materials to be explained was the origin of the small, positive θ_c which is, as mentioned, in sharp contrast to the cases of gadolinium and terbium titanate. Although consensus may not be fully established, there exists a very convincing argument from den Hertog and Gingras that the ferromagnetic coupling is the result of a dominant dipolar ferromagnetic term [45]. Calculations using the Ewald infinite summation method give a value for the dipolar term which exceeds the nearest neighbor exchange term, which is negative. Numerical simulations of the specific heat for $\text{Dy}_2\text{Ti}_2\text{O}_7$ on the dipolar spin ice model are in excellent agreement with experiment, as are calculated and observed neutron scattering patterns and magnetization data on single crystals in applied fields along high symmetry directions [44,46].

Predictions had been made for the stabilization of an ordered ground state or states in applied magnetic fields [47].

Neutron diffraction data at 0.35 K and applied fields up to 2.0 T show strong enhancement of reflections of the type (001), (002), (111) and (220), indicating a $k=0$ magnetic structure [36]. Interestingly, the application of high pressures fails to induce long range order in $\text{Ho}_2\text{Ti}_2\text{O}_7$, unlike the case of the spin liquid, $\text{Tb}_2\text{Ti}_2\text{O}_7$, suggesting a surprising robustness of the spin-ice ground state [32].

Spin-ice behavior has been confirmed in $\text{Ho}_2\text{Sn}_2\text{O}_7$ [48] and there are ac susceptibility results for the dysprosium stannate which also can be interpreted in this way [24]. For $\text{Dy}_2\text{Ti}_2\text{O}_7$ recent magnetization experiments on single crystals with the field applied in $\langle 111 \rangle$ directions have shown a field-induced phase transition from the spin ice state to a “three-spin-in, one-spin-out” state [49]. A similar phase transition is also found for a $[110]$ field direction [50].

6. $\text{Er}_2\text{Ti}_2\text{O}_7$ and $\text{Er}_2\text{Sn}_2\text{O}_7$

Evidence for long range magnetic order in $\text{Er}_2\text{Ti}_2\text{O}_7$ was found in the very earliest specific heat measurements of this material, in the form of a λ -peak at 1.25 K [13]. Thus, this material is neither a spin liquid nor a spin glass. Neutron diffraction in zero field has confirmed the long range order and a magnetic structure has been assigned (Fig. 17) [51]. The ordered moment of $3.01 \mu_B$ is consistent with the ground state Kramers doublet wavefunction and is strong evidence that the Er^{3+} moments lie in a plane normal to the $\langle 111 \rangle$ direction. Thus, $\text{Er}_2\text{Ti}_2\text{O}_7$ is an easy planar or XY magnet. Comparison of these results with early theory for the XY $\langle 111 \rangle$ pyrochlore magnet [52] exposes discrepancies. Principal of these is the observation of a continuous transition, whereas, theory

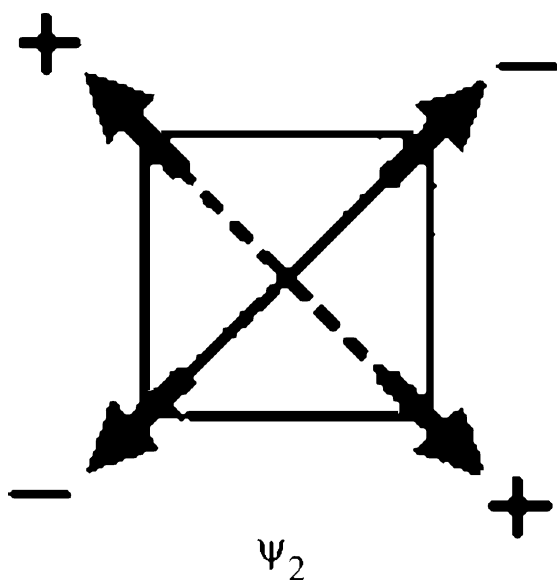


Fig. 17. Spin structure in the long range ordered state for $\text{Er}_2\text{Ti}_2\text{O}_7$ below $T_N = 1.173$ K [51]. A single tetrahedron is shown, viewed along a 2-fold axis.

predicts first order. There has been some speculation regarding the nature of the perturbation which breaks the enormous ground state degeneracy, selecting the specific ordered state observed. Both dipolar interactions and quantum fluctuations have been considered, with a preference for the latter. Thus, $\text{Er}_2\text{Ti}_2\text{O}_7$ has been proposed as an example of the “order by disorder” mechanism for selecting a unique ground state [51].

Surprisingly, $\text{Er}_2\text{Sn}_2\text{O}_7$ does not order down to 0.13 K nor does $\text{Er}_2\text{GaSbO}_7$ [13,24]. Once again, the extreme sensitivity of the ground state to apparently minor changes in materials chemistry is apparent.

7. $\text{Tm}_2\text{Ti}_2\text{O}_7$ and $\text{Tm}_2\text{Sn}_2\text{O}_7$

The thulium titanate pyrochlore is the least interesting of the series as the single ion ground state of Tm^{3+} , $^3\text{H}_6$, in the pyrochlore crystal field turns out to be a magnetic singlet [53]. Inelastic neutron scattering data show a first excited state at 10.6 meV (85 cm^{-1}) above the ground state. This is consistent with the set of crystal field parameters which have been developed for the pyrochlore titanates [16,54–56]. Similar behaviour is found for the corresponding stannate [24].

8. $\text{Yb}_2\text{Ti}_2\text{O}_7$ and $\text{Yb}_2\text{Sn}_2\text{O}_7$

$\text{Yb}_2\text{Ti}_2\text{O}_7$ was one of the first titanate pyrochlores to be studied in some detail. Susceptibility data over a very wide temperature range had been reported as early as 1964 and the very pronounced deviation from the Curie–Weiss law was attributed to the effect of the crystal field on the $^2\text{F}_{7/2}$ ground state [57]. A pronounced λ -peak at 0.25 K had long been interpreted as evidence for a transition to a long range ordered state [13]. Recent, intensive studies have established in detail the fundamental properties. Low temperature susceptibility and ^{170}Yb Mössbauer studies have established that the ground Kramers doublet is well isolated from the excited states and the observed Curie constant and g-factor are consistent with an easy planar moment orientation, as in $\text{Er}_2\text{Ti}_2\text{O}_7$ [58]. The Weiss constant is observed to be +0.75 K, ferromagnetic. Given the very small value of the Yb^{3+} moment, this can be ascribed to the nearest neighbor exchange rather than dipolar coupling.

Studies of the spin dynamics using ^{170}Yb Mössbauer and μSR have disclosed a truly remarkable, first order, decrease in the spin fluctuation rate by a factor of $\sim 10^4$ just at the temperature of the heat capacity anomaly (Fig. 18) [59]. Below 0.24 K the spin fluctuation rate is finite and constant. As well, neutron diffraction data show no new peaks in a difference plot between 0.11 and 7 K (Fig. 19) and no oscillations are observed in the μSR over a similar temperature range. Thus, from these studies there is no evidence of long range magnetic order below 0.24 K but a drastic slowing down of the spin

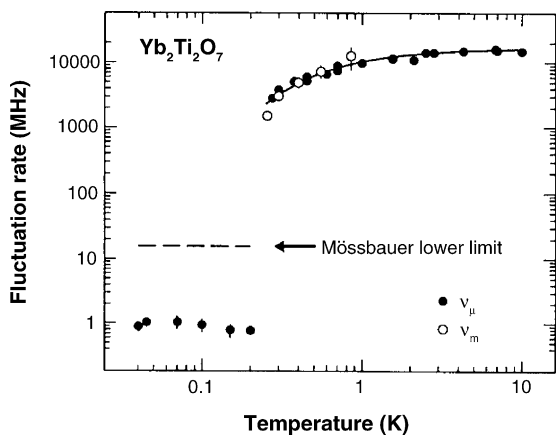


Fig. 18. The spin fluctuation rate for Yb^{3+} as a function of temperature as determined by ^{170}Yb Mossbauer spectroscopy and μSR . Note the first order change at the specific heat anomaly at 0.24 K [59].

fluctuations. An analogy has been drawn to the gas–liquid transition.

Nonetheless, a more recent neutron diffraction study finds evidence for ferromagnetic order at 0.03 K, in the form of the enhancement of the intensity of certain reflections (Fig. 20) [60]. The Yb moment deduced from the magnetic intensities is only $\sim 1 \mu_B$, which is considerably smaller than the expected value from the Kramers ground state wavefunction. This report is at variance with the most recent neutron data which extend to 0.04 K in which, again, no long range order is seen [26]. It is not clear how to reconcile these divergent results (Table 1).

Not surprisingly, much less is known about $\text{Yb}_2\text{Sn}_2\text{O}_7$. The bulk susceptibility is very similar to the titanate and for the ground crystal field state, $\theta_c = +0.51$, ferromagnetic as in the titanate [24].

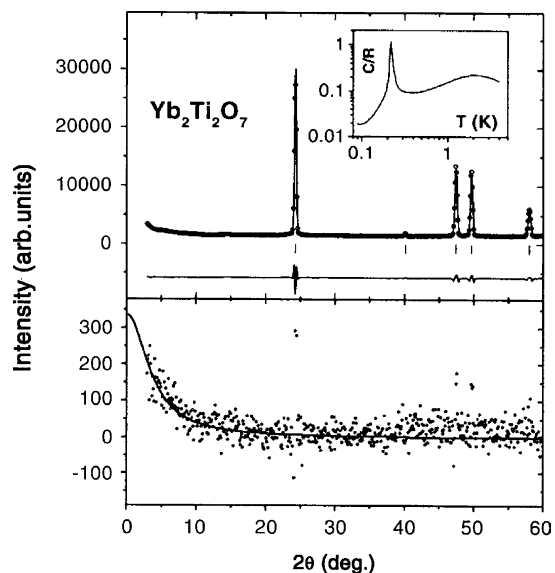


Fig. 19. Neutron diffraction data for $\text{Yb}_2\text{Ti}_2\text{O}_7$ at 7 K and the difference pattern for 0.11–7 K. No Bragg peaks are seen [59].

9. Comment on the stannate series

In the above, the similarities and differences between the corresponding titanate and stannate pyrochlores has been noted. As well, the crystal chemistry of the stannate series extends to larger rare earths, both $\text{Pr}_2\text{Sn}_2\text{O}_7$ and $\text{Nd}_2\text{Sn}_2\text{O}_7$ are stable as pyrochlores. Preliminary data suggest that the Pr phase may be a spin ice due to strong Ising-like character to the crystal field ground state [24]. The Nd stannate orders antiferromagnetically below 0.9 K [24]. This mimics behaviour of $\text{Nd}_2\text{GaSbO}_7$ [13].

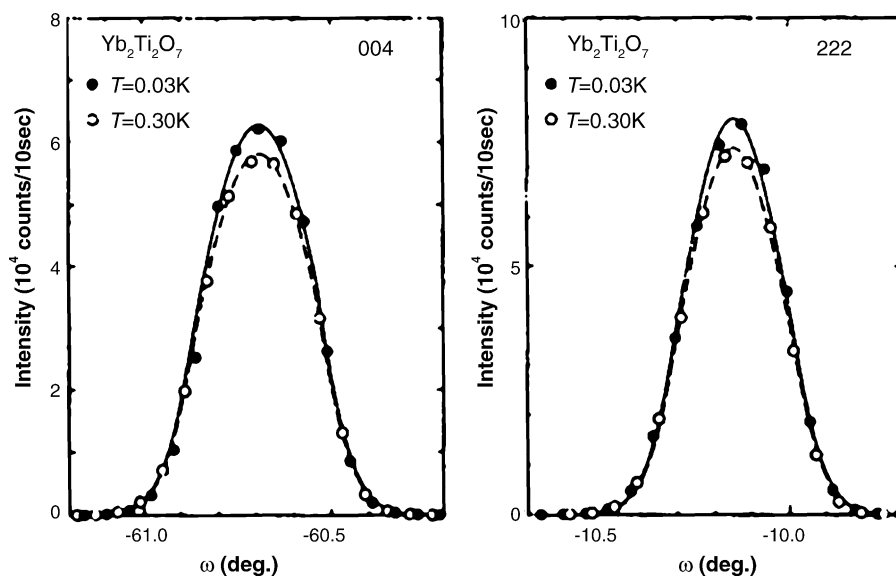


Fig. 20. Comparison of the intensities of the (004) and (222) reflections reflections at $T=0.30$ and 0.03 K, showing enhanced intensities at the lower temperature [60].

Table 1
Summary of the magnetic properties of the $R_2Ti_2O_7$ and $R_2Sn_2O_7$ pyrochlores

R	θ_c (K)	Exchange vs. dipolar	Anisotropy	Ground State	Orders in H or P
Pr(Sn)	0.32	?	Easy axis	Spin ice?	?, ?
Nd(Sn)	-0.31	?	?	AF, $T_N = 0.97$ K	–
Gd(Ti)	-9.6	Ex > D	~Isotropic	AF, $T_N = 0.9$ K, 0.6 K	Yes, ?
Gd(Sn)	-7	Ex > D	~Isotropic	AF, $T_N = 1.0$ K	–
Tb(Ti)	-19	Ex > D	Easy axis	Spin liquid	Yes, yes
Tb(Sn)	-12.5	Ex > D	?	?	?, ?
Dy(Ti)	1.2	D > Ex	Easy axis	Spin ice	Yes, ?
Dy(Sn)	1.7	D > Ex ?	Easy axis	Spin ice ?	?, ?
Ho(Ti)	1.9	D > Ex	Easy axis	Spin ice	Yes, no
Ho(Sn)	1.8	D > Ex	Easy axis	Spin ice	?, ?
Er(Ti)	-24	Ex > D	Easy plane	AF, $T_N = 1.24$ K	–
Er(Sn)	-14	Ex > D	Easy	Plane no order to 0.13 K	?, ?
Yb(Ti)	0.71	Ex > D	Easy plane	Spin liquid or F ?	?, ?
Yb(Sn)	0.51	Ex > D	Easy plane		?, ?

10. Summary and conclusions

Table 1 is an attempt to collect the known results and interpretations of the properties of the rare earth titanate and stannate pyrochlores.

Among the systematics shown, perhaps the exhibited anisotropy pattern, i.e. axial versus planar, is amenable to the most straightforward interpretation. This can be traced to the single ion properties of the rare earth ion with the assumption that the axial crystal field component, $B_0^2 C_0^2$, plays a determining role in the crystal field interaction. In fact, the systematics are more transparent if one uses, instead of the now standard tensor operator formalism, the Stevens operator equivalent approach [61]. Here the axial term is given as $B_0^2 O_0^2$, where O_0^2 is an operator equivalent equal to $3J_z^2 - J(J+1)$ and B_0^2 is a numerical factor equal to the product of, α_J , the Stevens multiplicative factor, and a factor expressing the electrostatic potential of the crystal field, A_0^2 . Since the sign of the crystal field potential will be the same for the rare earth site, independent of the identity of the rare earth, the sign of the product will depend on the sign of α_J . This factor is negative for Pr, Nd, Tb, Dy and Ho and is positive for Er, Tm and Yb. If B_0^2 is positive, the crystal field ground state will be comprised mainly of $|\pm M_J^{\min}\rangle$ components and for the opposite sign, $|\pm M_J^{\max}\rangle$ components. The former favours an easy planar anisotropy and the latter, an easy axis. From the table the variation in anisotropy within the rare earth titanate and stannate pyrochlores is consistent with the variation in the sign of α_J within the rare earth series.

It is considerably more difficult to understand the variation in the sign and magnitude of the nearest neighbor exchange which varies from strongly negative, Gd, Tb and Er, to weakly positive, Pr, Dy, Ho, Yb, with one case of a weakly negative exchange, Nd. The situation for the Er materials is also difficult to rationalize, as the titanate phase orders with $T_N > 1$ K while the stannate does not order to ~ 0.1 K.

From the large number of question marks decorating the above table, it is clear that much remains to be done to attain

a better understanding of the properties of these fascinating materials.

Acknowledgements

The Natural Sciences and Engineering Research Council of Canada has supported our research in geometrically frustrated magnetic materials over several years through the Discovery and Collaborative grant programs. The collaboration of many colleagues over the years is gratefully acknowledged, including A.J. Berlinsky, M. Bieringer, M.F. Collins, S. Dunsiger, J.S. Gardner, B.D. Gaulin, M.J.P. Gingras, R. Kiefl, G. Luke, N.P. Raju, J.N. Reimers, C.V. Stager, Y. Uemura, C.R. Wiebe, and A.S. Wills, among others.

References

- [1] A.P. Ramirez, Ann. Rev. Mater. Sci. 24 (1994) 453.
- [2] B.D. Gaulin, Hyperfine Inter. 85 (1994) 159.
- [3] P. Schiffer, A.P. Ramirez, Commun. Cond. Mater. Phys. 10 (1996) 21.
- [4] J.E. Greedan, J. Mater. Chem. 11 (2001) 37.
- [5] A.P. Ramirez, Handbook Magn. Mater. 13 (2001) 423.
- [6] S.T. Bramwell, M.J.P. Gingras, Science 294 (2001) 1495.
- [7] M.A. Subramanian, G. Aravamudan, G.V. Subba Rao, Prog. Solid State Chem. 15 (1983) 55.
- [8] M.A. Subramanian, A.W. Sleight, in: K.A. Gschneidner, L. Eyring (Eds.), Handbook on the Physics and Chemistry of Rare Earths, vol. 16, Elsevier Science Publishers, 1993, p. 225.
- [9] J.E. Greedan, in: H.P.J. Wijn (Ed.), Magnetic Properties of Non-Metals, vol. III/27, Springer-Verlag, Berlin, 1991, p. 100, Landolt-Bornstein, New Series.
- [10] J. Villain, Z. Phys. B33 (1979) 31.
- [11] J.N. Reimers, A.J. Berlinsky, A.-C. Shi, Phys. Rev. 43 (1991) 865; J.N. Reimers, Phys. Rev. 45 (1992) 7287.
- [12] R. Moessner, J.T. Chalker, Phys. Rev. Lett. 80 (1998) 2929; R. Moessner, J.T. Chalker, Phys. Rev. B58 (1998) 12049.
- [13] H.W.J. Blote, R.F. Wielinga, W.J. Huiskamp, Physica 43 (1969) 549.
- [14] J.D. Cashion, A.H. Cooke, A.H. Leask, M.J.N. Thorp, M.R. Wells, J. Mater. Sci. 3 (1968) 402.

- [15] N.P. Raju, M. Dion, M.J.P. Gingras, T.E. Mason, J.E. Greedan, *Phys. Rev. B* 59 (1999) 14489.
- [16] M.J.P. Gingras, B.C. den Hertog, M. Faucher, J.S. Gardner, S.R. Dunsiger, L.J. Chang, B.D. Gaulin, N.P. Raju, J.E. Greedan, *Phys. Rev. B* 62 (2000) 6496.
- [17] A.P. Ramirez, B.S. Shastry, A. Hayashi, J.J. Krajewski, D.A. Huse, R.J. Cava, *Phys. Rev. Lett.* 89 (2002) 067202.
- [18] J.D.M. Champion, A.S. Wills, T. Fennell, S.T. Bramwell, J.S. Gardner, M.A. Green, *Phys. Rev. B* 64 (2001) 140407R.
- [19] J.R. Stewart, G. Ehlers, A.S. Wills, S.T. Bramwell, J.S. Gardner, *J. Phys. Condens. Matter* 16 (2004) L321.
- [20] A.K. Hassan, L.P. Levy, C. Darie, P. Strobel, *Phys. Rev. B* 67 (2003) 214432.
- [21] O.A. Petrenko, M.R. Lees, G. Balakrishnan, D.M.K. Paul, *Phys. Rev. B* 70 (2004) 012402.
- [22] T. Katsufuji, H. Takagi, *Phys. Rev. B* 69 (2004) 064422.
- [23] O. Cepas, B.S. Shastry, *Phys. Rev. B* 69 (2004) 184402.
- [24] K. Matsuhira, Y. Hinatsu, K. Tenya, H. Amitsuka, T. Sakakibara, *J. Phys. Soc. Jpn.* 71 (2002) 1576.
- [25] P. Bonville, J.A. Hodges, M. Ocio, J.P. Sanchez, P. Vulliet, S. Sosin, D. Braithwaite, *J. Phys. Condens. Matter* 15 (2003) 7777.
- [26] P. Bonville, J.A. Hodges, E. Bertin, J.-Ph. Bouchard, M. Ocio, P. Dalmás de Reotier, L.-P. Regnault, H.M. Rønnow, J.P. Sanchez, S. Sosin, A. Yaouanc, M. Rams, K. Królas, LANL arXiv: cond-mat/0306470 v2.
- [27] J.S. Gardner, S.R. Dunsiger, B.D. Gaulin, M.J.P. Gingras, J.E. Greedan, R.F. Kiefl, M.D. Lumsden, W.A. MacFarlane, N.P. Raju, J.E. Sonier, I. Swainson, Z. Tun, *Phys. Rev. Lett.* 82 (1999) 1012.
- [28] J.S. Gardner, B.D. Gaulin, A.J. Berinsky, P. Waldron, S.R. Dunsiger, N.P. Raju, J.E. Greedan, *Phys. Rev. B* 64 (2001) 224416.
- [29] J.S. Gardner, A. Keren, G. Ehlers, C. Stock, E. Segal, J.M. Roper, B. Fak, M.B. Stone, P.R. Hammar, D.H. Reich, B.D. Gaulin, *Phys. Rev. B* 68 (2003) 180401.
- [30] A. Keren, J.S. Gardner, G. Ehlers, A. Fukaya, E. Segal, Y.J. Uemura, *Phys. Rev. Lett.* 92 (2004) 107204.
- [31] Y.-J. Kao, M. Enjalran, A. Del Maestro, H.R. Molavian, M.J.P. Gingras, *Phys. Rev. B* 68 (2003) 172407.
- [32] I. Mirabeau, I.N. Goncharenko, P. Cadavez-Peres, S.T. Bramwell, M.J.P. Gingras, J.S. Gardner, *Nature* 420 (2002) 54; I. Mirabeau, I.N. Goncharenko, *Physica B* 350 (2004) 250.
- [33] Y. Yasui, M. Kanada, M. Ito, H. Harashina, M. Sato, H. Okumura, K. Kakurai, *J. Phys. Chem. Solids* 62 (2001) 343.
- [34] G. Luo, S.T. Hess, L.R. Corruccini, *Phys. Lett. A* 291 (2001) 306.
- [35] N. Hamaguchi, T. Matsushita, N. Wada, Y. Yasui, M. Sato, *Phys. Rev. B* 69 (2004) 132413.
- [36] M.J. Harris, S.T. Bramwell, D.F. McMorrow, T. Zeiske, K.W. Godfrey, *Phys. Rev. Lett.* 79 (1997) 2554.
- [37] M.J. Harris, S.T. Bramwell, T. Zeiske, D.F. McMorrow, P.J.C. King, *J. Magn. Magn. Mater.* 177–181 (1998) 757.
- [38] S.T. Bramwell, M.J. Harris, *J. Phys. Condens. Matter* 10 (1998) 215.
- [39] W.F. Giaque, M.F. Ashley, *Phys. Rev.* 43 (1933) 81; W.F. Giaque, J.W. Stout, *J. Am. Chem. Soc.* 58 (1936) 1144.
- [40] D. Bernal, R.H. Fowler, *J. Chem. Phys.* 1 (1933) 515.
- [41] L. Pauling, *J. Am. Chem. Soc.* 57 (1935) 2680.
- [42] A.P. Ramirez, A. Hayashi, R.J. Cava, R. Siddharthan, B.S. Shastry, *Nature* 399 (1999) 333.
- [43] D.J. Flood, *J. Appl. Phys.* 45 (1974) 4041.
- [44] S.T. Bramwell, M.J. Harris, B.C. den Hertog, M.J.P. Gingras, J.S. Gardner, D.F. McMorrow, A.R. Wildes, A.L. Cornelius, J.D.M. Champion, R.G. Melko, T. Fennell, *Phys. Rev. Lett.* 87 (2001) 047205.
- [45] B.C. den Hertog, M.J.P. Gingras, *Phys. Rev. Lett.* 84 (2000).
- [46] H. Fukazawa, R.G. Melko, R. Higashinaka, Y. Maeno, M.J.P. Gingras, *Phys. Rev. B* 65 (2002) 054410.
- [47] R. Siddharthan, B.S. Shastry, A.P. Ramirez, *Phys. Rev. B* 63 (2001) 184412.
- [48] K. Matsuhira, Y. Hinatsu, K. Tenya, T. Sakakibara, *J. Phys. Condens. Matter* 12 (2000) 649.
- [49] T. Sakakibara, T. Tayama, Z. Hiroi, K. Matsuhira, S. Takagi, *Phys. Rev. Lett.* 90 (2003) 207205.
- [50] S. Yoshida, K. Nemoto, K. Wada, *J. Phys. Soc. Jpn.* 73 (2004) 1619.
- [51] J.D.M. Champion, M.J. Harris, P.C.W. Holdsworth, A.S. Wills, G. Balakrishnan, S.T. Bramwell, E. Čížmár, T. Fennell, J.S. Gardner, J. Lago, D.F. McMorrow, M. Orendáč, A. Orendáčová, D. McK. Paul, R.I. Smith, M.T.F. Welling, A. Wildes, *Phys. Rev. B* 68 (2003) 020401.
- [52] S.T. Bramwell, M.J.P. Gingras, J.N. Reimers, *J. Appl. Phys.* 75 (1994) 5523.
- [53] M.P. Zinkin, M.J. Harris, Z. Tun, R.A. Cowley, B.M. Wanklyn, *J. Phys. Condens. Matter* 8 (1996) 193.
- [54] Y.M. Jana, D. Ghosh, *Phys. Rev. B* 61 (2000) 9657; Y.M. Jana, A. Sengupta, D. Ghosh, *J. Magn. Magn. Mater.* 248 (2002) 7.
- [55] S. Rosenkranz, A.P. Ramirez, A. Hayashi, R.J. Cava, R. Siddharthan, B.S. Shastry, *J. Appl. Phys.* 87 (2000) 5914.
- [56] B.Z. Malkin, A.R. Zakirov, M.N. Popova, S.A. Klimin, E.P. Chukalina, E. Antic-Fidancev, Ph. Goldner, P. Aschehoug, G. Dhalenne, *Phys. Rev. B* 70 (2004) 075112.
- [57] M.G. Townsend, W.A. Crossley, *J. Phys. Chem. Solids* 29 (1968) 593.
- [58] J.A. Hodges, P. Bonville, A. Forget, M. Rams, K. Krolas, G. Dhalenne, *J. Phys. Condens. Matter* 13 (2001) 9301.
- [59] J.A. Hodges, P. Bonville, A. Forget, A. Yaouanc, P. Dalmás de Reotier, G. Andre, M. Rams, K. Krolas, C. Ritter, P.C.M. Gubbens, C.T. Kaiser, P.J.C. King, C. Baines, *Phys. Rev. Lett.* 88 (2002) 077204.
- [60] Y. Yasui, M. Soda, S. Iikubo, M. Ito, M. Sato, N. Hamaguchi, T. Matsushita, N. Wada, T. Takeguchi, N. Aso, K. Kakurai, *J. Phys. Soc. Jpn.* 72 (2003) 3014.
- [61] K.W.H. Stevens, *Proc. Phys. Soc. A* 65 (1952) 209.